Int. J. Heat Mass Transfer. Vol. 34, No. 1, pp. 47–53, 1991
Printed in Great Britain

0017-9310/91 \$3.00+0.00
Pergamon Press plc

# Heat transfer between a surface and a fluidized bed: consideration of pressure and temperature effects

V. A. BORODULYA, YU. S. TEPLITSKY, I. I. MARKEVICH, A. F. HASSAN and T. P. YERYOMENKO

Luikov Heat and Mass Transfer Institute, Minsk, 220728, U.S.S.R.

(*Received* 3 *January* 1989)

**Abstract**—A two-zone model of heat transfer between a fluidized bed and an immersed surface (*J. Engng Phys.* **56**(5), 767–773 (1989)) is used to correctly take into account the effect of the fluidized gas pressure and of the surface and bed temperatures on the overall heat transfer coefficient considered as the sum of conductive ($h_{\text{cond}}$), convective ($h_{\text{conv}}$) and radiative ($h_r$) components. The quantity $h_{\text{cond}}$ represents the effect of contact thermal conductivity of solid particles and also their convection near the heat transfer surface, $h_r$ takes account of the effect of the bed non-isothermicity near the surface on its effective emissivity. Based on the model used, correlations are obtained for computing the overall heat transfer coefficient. Comparison with the literature data shows that these correlations are valid over a wide range of experimental conditions: $0.1 \leqslant d \leqslant 6.0$ mm; $0.1 \leqslant p \leqslant 10.0$ MPa, $293 \leqslant T_\infty \leqslant 1713$ K; $293 \leqslant T_w \leqslant 1373$ K.

## INTRODUCTION

IN RECENT times a considerable amount of attention has been given to investigations in the sphere of fluidized bed combustion and gasification of solid fuels. The new technology has certain advantages over traditional techniques—a lower level of harmful emissions, a wider range of fuels being used, less cost of purification works, etc. The operating conditions of furnaces and reaction chambers of gas generators primarily involve high temperatures (1023–1173 K) of the bed and also increased pressures of the fluidizing gas (up to 2.0 MPa). Under such conditions, heat transfer between a fluidized bed and a surface has a complex conductive–convective–radiative character. Its rate depends on a great number of factors and their correct representation involves great difficulties the elimination of which first of all requires the elucidation of the mechanism of heat transfer and then the development of rather adequate models of combined heat transfer. For the most part the models available at present are rather specialized and, as a rule, describe a very limited body of experimental data on conductive–convective heat transfer [1–5]. The inclusion of radiative heat transfer is aggravated by the fact that there is no substantiated technique for calculating the fluidized bed effective emissivity [5] which would take into account the non-isothermicity of the bed near the heat transfer surface. One of the most well-known empirical formulae for calculating $h^{\max}$ is that of Baskakov and Panov [7] which predicts rather a strong dependence of the conductive component on pressure—the fact not confirmed experimentally [8]. Besides, this formula somewhat idealizes the effect of temperature $T_w$ on $h_r$, fully ignoring the bed temperature ($T_\infty$)—the fact which also lacks experimental confirmation [9].

In the present work attention is mostly paid to the functional dependence of the overall heat transfer coefficient on the governing parameters which reflects the effect of gas pressure and of the surface and bed temperatures on this coefficient and allows extremely wide generalizations of experimental data available in the literature.

## CONDUCTIVE–CONVECTIVE HEAT TRANSFER

The analysis of the process of conductive–convective heat transfer is made with use of the two-zone model [10] which presupposes the existence of an effective gas film at the heat transfer surface. Within the scope of this model [10] the following simple expression was obtained for $h_{\text{c-c}}$ in terms of the gas film characteristics:

$$h_{\text{c-c}} = \lambda_f^h / l_0. \tag{1}$$

The effective thermal conductivity and thickness of the film are defined as

$$\lambda_f^h = \lambda_f + 0.0061 \rho_f c_f \frac{u}{m} d \tag{2}$$

$$l_0 = 0.14 d (1-m)^{-2/3}. \tag{3}$$

The calculating formula for $h_{\text{c-c}}$, i.e.

$$Nu_{\text{c-c}} = 7.2(1-m)^{2/3} + 0.044 Re\, Pr \frac{(1-m)^{2/3}}{m} \tag{4}$$

which follows from equations (1) to (3), is used as the basis for obtaining the universal relations $Nu_{\text{c-c}}$ and $Nu_{\text{c-c}}^{\max}$.

## NOMENCLATURE

| | |
|---|---|
| $a$ | cylinder radius |
| $A$ | isothermicity parameter |
| $Ar$ | Archimedes number, $gd^3\rho_f(\rho_s-\rho_f)/\mu_f^2$ |
| $c$ | specific heat |
| $d_i$ | diameter of particles of $i$th fraction |
| $d$ | mean diameter of particles, $1/(\Sigma_i \eta_i/d_i)$ |
| $g$ | free fall acceleration |
| $H$ | bed height |
| $h$ | external heat transfer coefficient |
| $l_0$ | gas film thickness |
| $m$ | bed voidage |
| $Nu$ | Nusselt number, $hd/\lambda_f$ |
| $p$ | pressure |
| $Pe$ | Peclet number, $\rho_f c_f u l_0^2/Hm\lambda_f^0$ |
| $Pr$ | Prandtl number, $c_f\mu_f/\lambda_f$ |
| $Re$ | Reynolds number, $ud\rho_f/\mu_f$ |
| $T$ | temperature |
| $T_0$ | inlet gas temperature |
| $u$ | superficial velocity |
| $r$ | coordinate |
| $R$ | apparatus radius. |

Greek symbols

| | |
|---|---|
| $\varepsilon$ | emissivity |
| $\eta_i$ | mass fraction of particles with diameter $d_i$ |
| $\theta$ | dimensionless temperatures, $(T-T_0)/(T_w-T_0)$ |
| $\lambda$ | thermal conductivity |
| $\lambda_f^0$ | molecular thermal conductivity of gas at 273 K |
| $\Lambda$ | $\lambda_f^h/\lambda_f^0$ |
| $\mu$ | viscosity |
| $\xi$ | $r/R$ |
| $\rho$ | density |
| $\sigma$ | Stefan–Boltzmann constant |
| $\sigma^*$ | $\sigma/(1/\varepsilon_w+1/\varepsilon_c-1)$. |

Subscripts

| | |
|---|---|
| b | fluidized bed |
| cond | conductive |
| conv | convective |
| c–c | conductive–convective |
| e | effective |
| f | gas |
| mf | minimum fluidization |
| opt | optimum |
| r | radiative |
| s | solid particles |
| w | heat transfer surface |
| $\infty$ | fluidized bed core |
| $\Sigma$ | general. |

Superscripts

| | |
|---|---|
| h | horizontal |
| max | maximum |
| 0 | at $T = 273$ K |
| $\langle\ \rangle$ | at $T = (T_w+T_\infty)/2$. |

The analysis of the results of comparison between the experimental data for $h_{c\text{-}c}$ with those predicted by equation (4) showed that this formula satisfactorily describes only the experimental data for the beds of large particles ($d \geqslant 1$ mm). In the case of small particles, equation (4), as a rule, overpredicts the values of $h_{c\text{-}c}$. Heat transfer in the beds of small particles is mainly controlled by its conductive component which is defined by the expression $\lambda_f/l_0 = 7.2\lambda_f(1-m)^{2/3}/d$. The fact noted above indicates that $h_{c\text{-}c}$ does not depend so strongly on the diameter of particles. Therefore, the following correlation of the dependence of $l_0$ on $d$ was made:

$$l_0 = k_1\, Ar^{-k_2} d(1-m)^{-2/3}. \tag{5}$$

The non-linear dependence on $d$ is associated with the special features of motion of solid particles under the action of hydrodynamic forces near the heat transfer surface. As is seen, these features are taken into account by introducing into equation (5) the Archimedes number which is the generalized hydrodynamic characteristic of particles in a gas flow.

The generalization of the dependence of the gas film thermal conductivity on the determining parameters was made to correctly take into account the influence of the fluidizing gas pressure on the conductive component $h_{c\text{-}c}$. It turned out to be possible to realize by introducing into the expression for the conductive component $\lambda_f^h$ the simplexes $\lambda_s/\lambda_f$, $\rho_s/\rho_f$ and $c_s/c_f$ that represent the existence of the contact heat conduction between particles and their convection near the heat transfer surface

$$\lambda_f^h = k_3\lambda_f\left(\frac{\lambda_s}{\lambda_f}\right)^{k_4}\left(\frac{\rho_s}{\rho_f}\right)^{k_5}\left(\frac{c_s}{c_f}\right)^{k_6} + k_7\, Ar^{-k_2^*}\rho_f c_f\frac{u}{m}d. \tag{6}$$

In this equation, in the second term depending on $d$, the factor $Ar^{-k_2^*}$ takes account of the non-linear dependence of $\lambda_f^h$ on $d$. This is also due to the special character of the motion of particles near the heat transfer surface. Equations (5) and (6) together with equation (1) give

$$Nu_{c\text{-}c} = \frac{k_3}{k_1}Ar^{k_2}\left(\frac{\lambda_s}{\lambda_f}\right)^{k_4}\left(\frac{\rho_s}{\rho_f}\right)^{k_5}\left(\frac{c_s}{c_f}\right)^{k_6}(1-m)^{2/3} + \frac{k_7}{k_1}Ar^{k_2-k_2^*}\,Re\,Pr\frac{(1-m)^{2/3}}{m}. \tag{7}$$

For $Nu_{c\text{-}c}^{max}$ equation (7) yields

$$Nu_{c-c}^{max} = k_8\, Ar^{k'_2}\left(\frac{\lambda_s}{\lambda_f}\right)^{k'_4}\left(\frac{\rho_s}{\rho_f}\right)^{k'_5}\left(\frac{c_s}{c_f}\right)^{k'_6} + k_9\, Ar^{k_{10}}\, Pr. \quad (8)$$

The functional relationships given by equations (7) and (8) were used for wide generalizations of experimental data on conductive–convective heat transfer.

The values of the coefficients $k_i$ were found by comparison with literature experimental data. Reliable determination of the coefficient $k_i$ is already a challenge if only for the specificity of the structure of equations (7) and (8). Moreover, the solution of this problem is hindered by the familiar discrepancies in the determination of the $h_{c-c}$ coefficients by various authors (different measurement techniques, different types and dimensions of heat transfer surfaces, the specifics of the bed hydrodynamics, locations of probes, etc.). To hold the effect of these factors to a minimum, the coefficients $k_i$ were found in several steps.

Initially only the maximum values of the heat transfer coefficients were considered in beds of rather small particles ($d = 0.4$ mm) for the convective component $h_{c\text{-}c}$ to be neglected. The expression for $Nu_{cond}^{max}$ follows from equation (8)

$$Nu_{cond}^{max} = k_8\, Ar^{k'_2}\left(\frac{\lambda_s}{\lambda_f}\right)^{k'_4}\left(\frac{\rho_s}{\rho_f}\right)^{k'_5}\left(\frac{c_s}{c_f}\right)^{k'_6}. \quad (9)$$

The above equation is very convenient for analysis and, to determine the exponents in equation (9), allows one to use the simple and, as it turned out, rather an effective method that reduces to the minimum the errors in the determination of $k_i$ because of the above-noted discrepancies in the measurements of the heat transfer coefficient by different researchers. In the realization of this method use is made not of the absolute experimental values of $h_{cond}^{max}$, but rather of their ratios. Besides, the comparison is carried out under identical experimental conditions. Moreover, those experiments are selected in which the simplexes $\lambda_s/\lambda_f$, $\rho_s/\rho_f$ and $c_s/c_f$ have extremum values. This sufficiently expands the range of the results used and increases the reliability of determination of the coefficients $k'_i$. Considering this fact, the literature data selected (pp. 217, 307 and 469 of refs. [11–13], respectively) were used in the following form:

$$(h_{cond}^{max})_{copper}/(h_{cond}^{max})_{sand} = 1.27$$

(fluidizing medium—idem)

$$(h_{cond}^{max})_{lead}/(h_{cond}^{max})_{sand} = 1$$

(fluidizing medium—idem)

$$(h_{cond}^{max})_{helium}/(h_{cond}^{max})_{air} = 3$$

(particles—idem)

$$(h_{cond}^{max})_{hydrogen}/(h_{cond}^{max})_{air} = 3.45$$

(particles—idem). (10)

The substitution of equations (9) into equations (10) with the specific values of $\lambda$, $\rho$ and $c$ led to the system of four equations which after taking logarithms acquire the form

$$\begin{aligned} 1.27k'_2+3.02k'_4+1.27k'_5-0.72k'_6 &= 0.24\\ 1.51k'_2+3.85k'_4+1.51k'_5-1.81k'_6 &= 0\\ 1.9k'_2+1.7k'_4-1.9k'_5+1.66k'_6 &= 0.6\\ 1.16k'_2+1.94k'_4-2.6k'_5+2.66k'_6 &= 0.71. \end{aligned} \quad (11)$$

The solution of the system of linear algebraic equations (11) is $k'_2 = 0.16$; $k'_4 = 0.03$; $k'_5 = 0.14$; $k'_6 = 0.30$. The suitability of these values of $k'_i$ for describing experiments under different conditions was confirmed by the results of generalization of literature data [2–4, 8, 14–20] by relation (8) which involved the values of $k'_i$ obtained

$$Nu_{c\text{-}c}^{max} = 0.4Ar^{0.16}\left(\frac{\rho_s}{\rho_f}\right)^{0.14}\left(\frac{c_s}{c_f}\right)^{0.30} + 0.0013Ar^{0.63}\,Pr. \quad (12)$$

Due to the exponent of the simplex $\lambda_s/\lambda_f$ being small, the latter was ignored when the experimental data were processed. Equation (12) is valid in the following range of parameters: $0.1 \leqslant d \leqslant 4.0$ mm; $0.1 \leqslant p \leqslant 10$ MPa ($1.4\times10^2 \leqslant Ar \leqslant 1.11\times10^7$). The standard deviation of experimental points from those predicted by equation (12) amounts to 14% (Fig. 1). As is seen, the exponents of $Ar$ and $\rho_s/\rho_f$ being almost equal, the dependence of the conductive component of the coefficient $h_{c\text{-}c}$ on pressure is very weak. This corresponds to the well-known experimental fact of the weak dependence of the conductive–convective heat transfer coefficient on pressure beds of small particles [8].

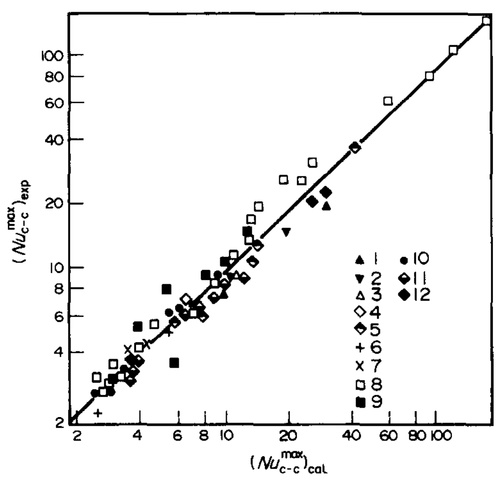


FIG. 1. Comparison between experimental data of refs. [2–4, 8, 14–20] and the results predicted by equation (12). 1, ref. [4] ($d = 1.3$; 4 mm); 2, ref. [2] ($d = 2$; 3 mm); 3, ref. [3] ($d = 1.6$ mm); 4, ref. [14] ($d = 0.7$ mm); 5, ref. [15] ($d = 0.25$; 0.62; 0.98 mm); 6, ref. [16] ($d = 0.1$; 0.4 mm); 7, ref. [17] ($d = 0.26$; 0.35 mm); 8, ref. [8] ($d = 0.126$; 1.22 mm; $p = 0.1$–8.1 MPa); 9, ref. [18] ($d = 0.75$; 1.5 mm; $p = 0.5$–10.0 MPa); 10, ref. [19] ($d = 0.12$–1.16 mm); 11, 12, ref. [20] ($d = 0.16$–2.37 mm; $p = 0.1$–0.93 MPa). 1–7, 10, at atmospheric pressure.

The determination of exponents in equation (7) was also carried out in a few steps. Firstly, only experimental data on heat transfer of a single horizontal tube in beds at atmospheric pressure and low temperatures were correlated when the values of the simplexes $\lambda_s/\lambda_f$, $\rho_s/\rho_f$ and $c_s/c_f$ vary only slightly. This allowed one to rather reliably reveal the dependence of $h_{c\text{-}c}$ on $Ar$ (on the diameter of particles). Correlation of the experimental data of refs. [2–4, 14–17] on the basis of equation (7) without inclusion of the simplexes $\lambda_s/\lambda_f$, $\rho_s/\rho_f$, $c_s/c_f$ gave

$$Nu_{c\text{-}c} = 2.62Ar^{0.1}(1-m)^{2/3}+0.033Re\,Pr\frac{(1-m)^{2/3}}{m}. \tag{13}$$

Equation (13) describes experimental data with the mean-square error of 17% (Fig. 2). It was checked in the following range of $Ar$: $1.4\times10^2$–$6.8\times10^6$ ($d = 0.1$–$4.0$ mm). The mean bed voidage was calculated from the familiar relations [10].

The second step in the calculation of the values of $k_i$ in equation (7) was the use of experimental data at evaluated pressures [8, 18]. The generalization of the sampling of experimental data on the values of $h_{c\text{-}c}$ [2–4, 8, 14–18] was carried out on the basis of equation (7). In this case it was assumed that $k_2 = 0.1$; $k_4 = 0$; $k_6 = k_2+k_5 = 0.1+k_5$. The latter assumption agrees with the results of determination of the coefficients $k_i'$ in equation (8) where it was obtained that $k_6' = k_2'+k_5'$. Moreover, it follows from purely physical considerations that it is reasonable to use not specific, but rather volumetric heat capacities, because it is precisely these qualities that enter into the corresponding heat conduction equations. As $Ar$ includes the factor $\rho_s/\rho_f - 1 \approx \rho_s/\rho_f$, the condition $k_6 = k_2+k_5$ leads to the appearance of the physically justified factor $(\rho_s c_s/\rho_f c_f)^{0.1+k_5}$ in the expression for the conductive component $h_{c\text{-}c}$. The generalization of the above-mentioned experimental data on the quantity $h_{c\text{-}c}$ gave the following correlation:

$$Nu_{c\text{-}c} = 0.74Ar^{0.1}\left(\frac{\rho_s}{\rho_f}\right)^{0.14}\left(\frac{c_s}{c_f}\right)^{0.24}(1-m)^{2/3} +0.46Re\,Pr\frac{(1-m)^{2/3}}{m} \tag{14}$$

which generalized the experimental values of $h_{c\text{-}c}$ with the mean-square error of 22% (Fig. 3). Equation (14) was checked in the following ranges: $0.1 \leqslant d \leqslant 4.0$ mm; $0.1 \leqslant p \leqslant 10.0$ MPa ($1.4\times10^2 \leqslant Ar \leqslant 1.1\times10^7$).

On the basis of equation (14) and with the use of the condition $dNu_{c\text{-}c}/dRe = 0$, the values of $Re_{opt}$ were calculated at which the maximum value of $Nu_{c\text{-}c}$ is attained. Rather a weak dependence of $Re_{opt}$ on $\rho_s/\rho_f$ and $c_s/c_f$ allowed the approximation of the $Re_{opt}$ values by the following relation:

$$Re_{opt} = 0.093Ar^{0.57} \tag{14a}$$

which in the range $10^2 \leqslant Ar \leqslant 10^7$ is in a good agreement with the well-known Todes formula [13] (the standard deviation does not exceed 15%).

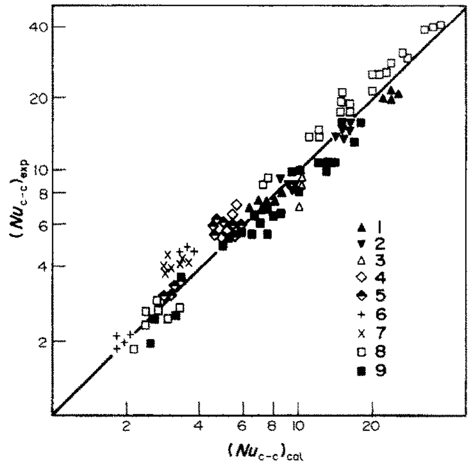


FIG. 3. Comparison between experimental data of refs. [2–4, 8, 14–18] and the results predicted by equation (14). 1–9, see Fig. 1.

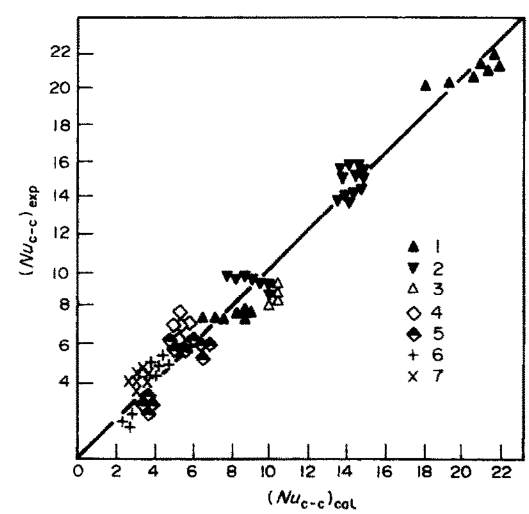


FIG. 2. Comparison between experimental data of refs. [2–4, 14–17] and the results predicted by equation (13). 1–7, see Fig. 1.

## CONDUCTIVE–CONVECTIVE–RADIATIVE HEAT TRANSFER

In the first place it is necessary to obtain the determining temperature for calculating the physical characteristics of the gas under the conditions of radiation effect. This can be easily done on the basis of the heat transfer model used. Considering the gas interlayer to be transparent for radiation and also taking into account that in a developed fluidized bed the heat transfer is limited only by the gas film resistance near the heat transfer surface, the system of equations for modelling the heat transfer of a vertical tube with a high-temperature bed has the form

$$\frac{1}{\xi}\frac{\mathrm{d}}{\mathrm{d}\xi}\left(\Lambda(\theta_{\mathrm{f}}^{k})\xi\frac{\mathrm{d}\theta_{\mathrm{f}}^{k}}{\mathrm{d}\xi}\right) = Pe\,\theta_{\mathrm{f}}^{k} \tag{15}$$

$$(a/l_0 \leqslant \xi \leqslant 1+a/l_0)$$

$$\theta_{\mathrm{f}}^{k}(a/l_0) = 1;\quad \theta_{\mathrm{f}}^{k}(1+a/l_0) = \infty \tag{16}$$

with the additional condition

$$-\frac{\lambda_{\mathrm{f}}^{\mathrm{h}}(T_\infty)(T_{\mathrm{w}}-T_0^{k-1})}{l_0}\frac{\mathrm{d}\theta_{\mathrm{f}}^{k-1}}{\mathrm{d}\xi} - \sigma^*(T_\infty^4 - T_{\mathrm{w}}^4) = \frac{\rho_{\mathrm{f}}c_{\mathrm{f}}u(T_\infty - T_0^k)}{H}\frac{R^2-a^2}{2a} \tag{17}$$

which determines the temperature of the incoming gas ($T_0$). The system of equations (15) and (16) was solved numerically by the time-dependent technique from the corresponding non-stationary problem. Since $\theta_{\mathrm{f}}^{k}$ is a function of $T_0^k$, the solution of equations (15) and (16) is first found for the given initial approximation $T_0^0$. Each subsequent $T_0^k$, necessary for the determination of $\theta_{\mathrm{f}}^{k}$ from equations (15) and (16), was found from equation (17). The process of iteration on the quantities $T_{\mathrm{f}}^{k}$ and $T_0^k$ terminated when $|(T_0^k - T_0^{k-1})/T_0^k| \leqslant 10^{-5}$. Calculations were made for $d = $ 1–6 mm, $T_{\mathrm{w}}$, $T_\infty = $ 873–1473 K. It is found that the value of the coefficient $h_\Sigma$, determined from equations (15) and (16) by the formula

$$h_\Sigma = \frac{\lambda_{\mathrm{f}}^{\mathrm{h}}(T_{\mathrm{f}}(a))}{T_\infty - T_{\mathrm{w}}}\frac{\mathrm{d}T_{\mathrm{f}}(a)}{\mathrm{d}r} + \frac{\sigma^*(T_\infty^4 - T_{\mathrm{w}}^4)}{T_\infty - T_{\mathrm{w}}} \tag{18}$$

coincides within 1% with the value of $h_\Sigma$ obtained from the solution of the system of equations (15) and (16) at $Pe = 0$ (for the conditions of the fluidized-bed furnace operation the value of $Pe$ does not exceed 0.4).

The results of the numerical experiment allow one to use the system of equations (15) and (16) with $Pe = 0$ for the analysis of the specific features of combined heat transfer. At $\lambda_{\mathrm{f}}^{\mathrm{h}} \simeq (\lambda_{\mathrm{f}}^{\mathrm{h}})^0 + B(T_{\mathrm{f}} - 273)$ it admits a simple analytical solution [21] which gives the following expression for $h_\Sigma$:

$$h_\Sigma = \frac{\langle\lambda_{\mathrm{f}}^{\mathrm{h}}\rangle}{l_0} + \sigma^*(T_\infty^2 + T_{\mathrm{w}}^2)(T_\infty + T_{\mathrm{w}}). \tag{19}$$

The actual dependence of $\lambda_{\mathrm{f}}^{\mathrm{h}}$ on $T_{\mathrm{f}}$ is not strictly linear, therefore equation (19) should be considered as a reasonable approximation.

As is known, the problem of correct representation of radiative heat transfer within the scope of equation (19) reduces to the determination of the effective emissivity of a fluidized bed ($\varepsilon_{\mathrm{e}}$) which enters into the quantity $\sigma^*$ and which takes into account the effect of the bed non-isothermicity near the heat transfer surface. The functional dependence of $\varepsilon_{\mathrm{e}}$ on the temperatures of the bed core ($T_\infty$) and the heat transfer surface ($T_{\mathrm{w}}$) was found in ref. [8]

$$\frac{\varepsilon_{\mathrm{e}}}{\varepsilon_{\mathrm{b}}} = A + (1-A)\left(\frac{T_{\mathrm{w}}}{T_\infty}\right)^4,\quad \left(\frac{T_{\mathrm{w}}}{T_\infty} \leqslant 1\right). \tag{20}$$

Equation (20) was used to correlate the data of ref. [6] on $\varepsilon_{\mathrm{e}}$ measured in a fluidized bed of corundum. To calculate the coefficient $A$ (the parameter of isothermicity), it was obtained that

$$A = 1 - \exp(-0.16Ar^{0.26}),\quad Ar \geqslant 1.22\times 10^2 \tag{21}$$

where the values of $Ar$ were calculated at the temperature $T_\infty$. From equation (21) it follows that with $Ar \geqslant 10^5$ the isothermicity parameter is $A \approx 1$ and $\varepsilon_{\mathrm{e}} \approx \varepsilon_{\mathrm{b}}$—the case fully corresponding to an isothermal bed. The result obtained agreed with the conclusions of ref. [22] where it was shown that intensive interphase heat transfer in the beds of particles with $d \geqslant 1$ mm greatly compensates heat losses by particles due to heat conduction to the wall. The experimental data of ref. [23] on heat transfer of chamotte particles at high temperatures also indicates insignificant cooling of particles with $d > 1$ mm and the necessity of taking this effect into account in the beds of small ($d \leqslant 0.5$ mm) particles.

The generalization of experimental data of refs. [2, 4, 6, 8, 14–18, 24], including also the experiments at high temperatures [6, 24], on the basis of equations (14) and (19) led to the following correlation:

$$Nu_\Sigma = 0.85Ar^{0.1}\left(\frac{\rho_{\mathrm{s}}}{\rho_{\mathrm{f}}}\right)^{0.14}\left(\frac{c_{\mathrm{s}}}{c_{\mathrm{f}}}\right)^{0.24}(1-m)^{2/3} + 0.046Re\,Pr\frac{(1-m)^{2/3}}{m} + \frac{d}{\langle\lambda_{\mathrm{f}}\rangle}\sigma^*(T_\infty^2 + T_{\mathrm{w}}^2)(T_\infty + T_{\mathrm{w}}). \tag{22}$$

This relation generalizes the above-indicated experimental data with the mean-square error of 18% (Fig. 4) and is valid within the ranges: $0.10 \leqslant d \leqslant 6.0$ mm;

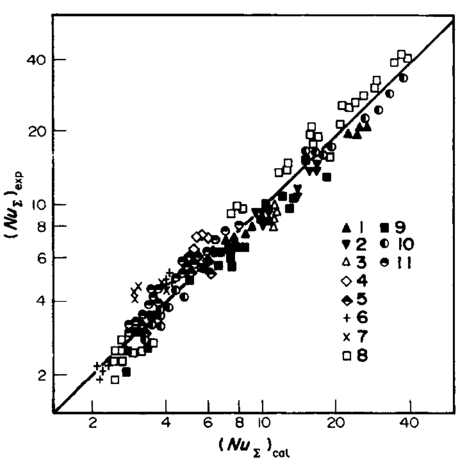


FIG. 4. Comparison between experimental data of refs. [2–4, 6, 8, 14–18, 24] and the results predicted by equation (22). 1–9, see Fig. 1; 10, ref. [6] ($d = 0.5$; 6 mm; $p = 0.1$ MPa; $T_{\mathrm{w}} = $ 273–1373 K; $T_\infty = $ 1073; 1473 K); 11, ref. [24] ($d = 0.35$; 0.63; 1.25 mm; $p = 0.1$ MPa; $T_{\mathrm{w}} = $ 433–1023 K; $T_\infty = $ 1123 K).

$0.1 \leqslant p \leqslant 10.0$ MPa; $293 \leqslant T_\infty \leqslant 1473$ K; $293 \leqslant T_w \leqslant 1373$ K ($1.4\times10^2 \leqslant Ar \leqslant 1.1\times10^7$).

The result of an analogous correlation of experimental data on the maximum heat transfer coefficients [2–4, 6, 8, 9, 14–20, 23–28] on the basis of equations (12) and (19) is

$$Nu_\Sigma^{max} = 0.36Ar^{0.16}\left(\frac{\rho_s}{\rho_f}\right)^{0.14}\left(\frac{c_s}{c_f}\right)^{0.30} + 0.0013Ar^{0.63}\,Pr + \frac{d}{\langle\lambda_f\rangle}\sigma^*(T_\infty^2+T_w^2)(T_\infty+T_w). \quad (23)$$

Correlation (23) is checked under the following conditions: $0.1 \leqslant d \leqslant 6.0$ mm; $0.1 \leqslant p \leqslant 10.0$ MPa; $293 \leqslant T_\infty \leqslant 1713$ K; $293 \leqslant T_w \leqslant 1373$ K ($1.4\times10^2 \leqslant Ar \leqslant 1.1\times10^7$). It describes the experimental data with the mean-square error of 16% (Fig. 5). The values of the thermophysical characteristics of phases in equations (22) and (23) are taken at a mean temperature $[(T_\infty+T_w)/2]$. The emissivity of an isothermal bed in the expression for $\sigma^*$ is calculated by the formula [29]

$$\varepsilon_b = 1.63\frac{m-m_{mf}}{1-m_{mf}}\varepsilon_s^{0.310} + \left(1-1.63\frac{m-m_{mf}}{1-m_{mf}}\right)\varepsilon_s^{0.485}. \quad (24)$$

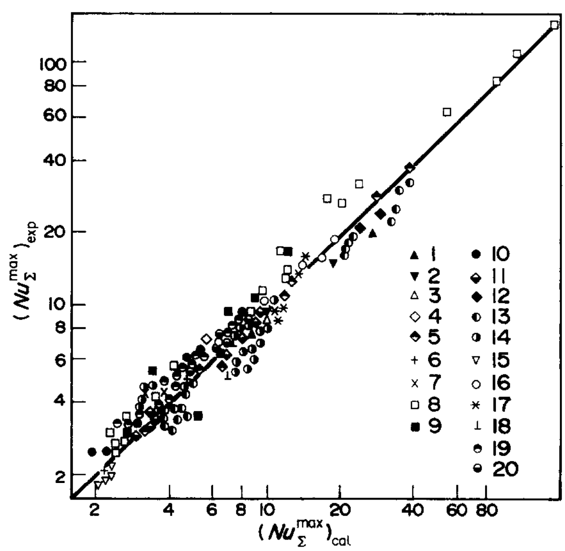


FIG. 5. Comparison between experimental data of refs. [2–4, 6, 8, 9, 14–20, 23–28] and the results predicted by equation (23). 1–12, see Fig. 1; 13, ref. [6] (see Fig. 4); 14, ref. [25] ($d = 0.34$–$1.66$ mm; $p = 0.1$ MPa; $T_w = 423$–$573$ K; $T_\infty = 573$–$1173$ K); 15, ref. [26] ($d = 0.12$; 0.32 mm; $p = 0.1$ MPa; $T_w = 373$–$423$ K; $T_\infty = 473$–$673$ K); 16, ref. [9] ($d = 1.05$–$4$ mm); $p = 0.1$ MPa; $T_w = 303$ K; $T_\infty = 1073$–$1273$ K); 17, ref. [23] ($d = 1.22$; 1.73 mm; $p = 0.1$ MPa; $T_w = 423$–$1573$ K); $T_\infty = 1223$–$1573$ K); 18, ref. [28] ($d = 0.37$; 1.25 mm; $p = 0.1$ MPa; $T_w = 337$–$628$ K; $T_\infty = 573$–$1273$ K); 19, ref. [24] (see Fig. 4); 20, ref. [27] ($d = 0.8$; 1.3; 1.8 mm; $p = 0.1$ MPa; $T_w = 373$ K; $T_\infty = 753$–$1713$ K).

In the case of polyfractional particles, the heat transfer coefficients are calculated with the use of the equivalent diameter of particles determined from the formula

$$d = 1\Big/\sum_i (\eta_i/d_i).$$

## CONCLUSION

Based on the two-zone model, an analysis of the process of combined heat transfer in a fluidized bed is carried out. The correct representation of the influence of pressure, bed temperatures and of the heat transfer surface on $h_\Sigma$ and $h_\Sigma^{max}$ is made. The effect of the bed non-isothermicity on the magnitude of the radiative component of heat transfer coefficient is taken into account. Relations (22) and (23) derived are checked over extremely wide ranges of experimental conditions and can be used for calculating heat transfer in fluidized-bed and gas generators.

## REFERENCES

1. V. L. Ganzha, S. N. Upadhyay and S. C. Saxena, A mechanistic theory for heat transfer between fluidized beds of large particles and immersed surfaces, *Int. J. Heat Mass Transfer* **25,** 1531–1540 (1982).
2. S. S. Zabrodsky, Yu. G. Epanov, D. M. Galerstein, S. C. Saxena and A. K. Holar, Heat transfer in a large-particle fluidized bed with immersed in-line and staggered bundles of horizontal smooth tubes, *Int. J. Heat Mass Transfer* **24,** 571–579 (1981).
3. F. W. Staub, Solids circulation in turbulent fluidized beds and heat transfer to immersed tube banks, *J. Heat Transfer* **101,** 391–396 (1979).
4. N. M. Catipovic, Heat transfer to horizontal tubes in fluidized beds: experiment and theory, Ph.D. Thesis, Oregon State University, Corvallis, Oregon (1979).
5. N. Decker and L. R. Glicksman, Heat transfer in large-particle fluidized beds, *Int. J. Heat Mass Transfer* **26,** 1307–1320 (1983).
6. O. M. Panov, A. P. Baskakov, Yu. M. Goldobin, N. F. Filippovsky and Yu. S. Mazur, An experimental study of radial and conductive–convective component of external heat transfer in a high-temperature fluidized bed, *J. Engng Phys.* **36**(3), 409–415 (1979).
7. A. P. Baskakov and O. M. Panov, Comparison of maximum coefficients of heat transfer to a surface submerged in a fluidized bed with an estimate obtained from an empirical formula, *J. Engng Phys.* **45**(6), 896–901 (1973).
8. V. A. Borodulya, V. L. Ganzha and V. I. Kovenskiy, *Hydrodynamics and Heat Transfer in a Pressurized Fluidized Bed.* Izd. Nauka i Tekhnika, Minsk (1982).
9. V. A. Borodulya, Yu. S. Teplitsky, A. P. Sorokin, V. V. Matsnev, I. I. Markevich and V. I. Kovenskiy, External heat transfer in polydispersed fluidized beds at increased temperatures, *J. Engng Phys.* **56**(5), 767–773 (1989).
10. V. A. Borodulya, V. L. Ganzha, Yu. S. Teplitsky and Yu. G. Epanov, Heat transfer in fluidized beds, *J. Engng Phys.* **49**(4), 621–626 (1985).
11. J. S. M. Botterill, *Fluid-bed Transfer Gas-fluidized Bed Behaviour and its Influence on Bed Thermal Properties.* Academic Press, London (1975).
12. N. I. Gelperin, V. G. Ainstein and V. B. Kvasha,

*Fundamentals of Fluidization Technique*. Izd. Khimiya, Moscow (1967).
13. M. E. Aerov and O. M. Todes, *Hydraulic and Thermal Foundations of the Operation of Steady-state and Fluidized Granular Bed Apparatuses*. Izd. Khimiya, Leningrad (1968).
14. B. Nenkirchen and H. Blenke, Gestaltung horizontaler Rohrbündel in Gas-Wirblschichtreaktoren nach wärmetechnischen Gesichtspunkten, *Chemie-Ingr-Tech.* **45**(5), 307–312 (1973).
15. G. I. Pal'chyonok, Characteristics of heat and mass transfer to the movable and fixed surface in fluidized bed and techniques of their calculating available to combustion of solid fuel, Author's abstract of candidate thesis, Minsk (1984).
16. A. P. Baskakov and G. K. Malikov, Determination of heat transfer coefficients from the damaged bed to the cylindrical heat probe, *Khim. Prom.* No. 6, 27–28 (1966).
17. N. I. Gelperin, V. G. Ainstein and A. V. Zaikovskiy, Concerning the mechanism of heat transfer between a surface and non-uniform granular bed, *Khim. Prom.* No. 6, 18–26 (1966).
18. D. G. Traber, V. M. Pomerantsev, I. P. Mukhlenov and V. B. Sarkits, Heat transfer from suspended bed of catalyzer to the heat transfer surface, *Zh. Prikl. Khim.* **35**, 2386–2393 (1962).
19. N. N. Varygin and I. G. Martyushin, Calculation of the heat transfer surface in fluidized bed apparatuses, *Khim. Mashinostr.* No. 5, 6–9 (1959).
20. A. O. Denloye and J. S. M. Botterill, Bed to surface heat transfer in a fluidized bed of large particles, *Powder Technol.* **19**, 197–203 (1978).
21. V. P. Isachenko, V. A. Osipova and A. S. Sukomel, *Heat Transfer*. Energoizdat, Moscow (1981).
22. V. A. Borodulya and V. I. Kovenskiy, Concerning the packet model of external heat transfer for a fluidized bed, *J. Engng Phys.* **47**(5), 789–796 (1984).
23. K. Ye. Makhorin, V. S. Pikashov and G. P. Kuchin, Heat transfer between fluidized particles and the surface, *Khim. Tekhnol.* No. 2, 41–44 (1976).
24. A. P. Baskakov and Yu. M. Goldobin, Radiative heat transfer in a gas-fluidized bed, *Izv. Akad. Nauk SSSR, Energetika Transport* No. 4, 163–168 (1970).
25. N. V. Kharchenko and K. Ye. Makhorin, Concerning the heat transfer rate between a fluidized bed and a submerged body at high temperatures, *J. Engng Phys.* **7**(5), 12–17 (1964).
26. Yu. I. Alekseyev, N. F. Filippovskiy, A. P. Baskakov, V. A. Dedykhin and A. I. Poryvkin, Study of heat exchange in a bed fluidized with steam, *J. Engng Phys.* **42**(6), 898–902 (1982).
27. A. T. Tishchenko and Yu. I. Khvastukhin, The effect of temperature on heat transfer between fluidized bed and the surface placed in it, *Khim. Prom.* No. 6, 445–447 (1967).
28. K. Ye. Makhorin, V. S. Pikashov and G. P. Kuchin, *Heat Transfer in a High-temperature Boiling Bed*. Izd. Naukova Dumka, Kiev (1981).
29. V. I. Kovenskiy, Calculation of the emittance of a disperse system, *J. Engng Phys.* **38**(6), 983–988 (1980).

## TRANSFERT THERMIQUE ENTRE UNE SURFACE ET UN LIT FLUIDISE: EFFETS DE LA PRESSION ET DE LA TEMPERATURE

**Résumé**—Un modèle bidimensionnel de transfert thermique entre un lit fluidisé et une surface immergée (*J. Engng Phys.* **56**(5), 767–773 (1989)) est utilisé pour prendre correctement en compte l'effet de la pression du gaz et de la surface et des températures sur le coefficient global de transfert considéré comme la somme des composants conductif ($h_{cond}$), convectif ($h_{conv}$) et radiatif ($h_r$). La grandeur $h_{cond}$ représente l'effet de la conductivité thermique de contact des particules solides et aussi leur convection près de la surface; $h_r$ prend en compte l'effet de la non isothermicité du lit près de la surface sur l'émissivité effective. A partir du modèle, on obtient des formules pour calculer le coefficient global de transfert de chaleur. Une comparaison avec les données disponibles montre que ces formules sont valables dans un large domaine de conditions expérimentales: $0{,}1 \leqslant d \leqslant 6{,}0$ mm; $0{,}1 \leqslant p \leqslant 10$ MPa; $293 \leqslant T_\infty \leqslant 1713$ K; $293 \leqslant T_w \leqslant 1373$ K.

## WÄRMEÜBERGANG AN EINER OBERFLÄCHE IN EINEM WIRBELBETT—EINFLUSS VON DRUCK UND TEMPERATUR

**Zusammenfassung**—Der Wärmeübergang an einer Oberfläche in einem Wirbelbett wird mit Hilfe eines 2-Zonen-Modells (*J. Engng Phys.* **56**(5), 767–773 (1989)) untersucht. Dadurch ist es möglich, den Einfluß des Druckes und der Temperaturen von Oberfläche und Wirbelbett auf den Gesamtwärmeübergangskoeffizienten korrekt zu berücksichtigen. Dieser Koeffizient wird als Summe von Wärmeleitungs-, Konvektions- und Strahlungs-Beiträgen betrachtet. Der Wärmeleitungsanteil enthält die Einflüsse des Kontaktwiderstandes zwischen den Feststoffpartikeln wie auch deren Konvektion nahe an der wärmeübertragenden Oberfläche. Im Strahlungsbeitrag wird der Einfluß ungleichförmiger Wirbelbettemperatur nahe der Oberfläche auf das effektive Emissionsvermögen berücksichtigt. Mit Hilfe des verwendeten Modells ergeben sich Korrelationsgleichungen zur Berechnung des Gesamtwärmeübergangskoeffizienten. Ein Vergleich mit Angaben aus der Literatur zeigt, daß diese Korrelationen über einen weiten Bereich von Versuchsbedingungen gültig sind: $0{,}1 \leqslant d \leqslant 6{,}0$ mm; $0{,}1 \leqslant p \leqslant 10{,}0$ MPa; $293 \leqslant T_\infty \leqslant 1713$ K; $293 \leqslant T_w \leqslant 1373$ K.

## ЗАКОНОМЕРНОСТИ ТЕПЛООБМЕНА МЕЖДУ ПОВЕРХНОСТЬЮ И ПСЕВДООЖИЖЕННЫМ СЛОЕМ: УЧЕТ ВЛИЯНИЯ ДАВЛЕНИЯ И ТЕМПЕРАТУРЫ

**Аннотация**—Двухзонная модель теплообмена между псевдоожиженным слоем и погруженной в него поверхностью (*J. Engng Phys.* **56**(5), 767–773 (1989)) используется для корректного учета влияния давления давления ожижающего газа, температур поверхности и слоя на величину полного коэффициента теплообмена, рассматриваемого как сумма кондуктивной ($h_{cond}$), конвективной ($h_{conv}$) и радиационной ($h_r$) составляющих. Величина $h_{cond}$ учитывает влияние контактной теплопроводности твердых частиц, а также их конвекцию у теплообменной поверхндсти, $h_r$ учитывает влияние неизотермичности слоя у поверхности на его эффективную степень черноты. На основе использованной модели получены корреляции для расчета полного коэффициента теплообмена. Сравнение с литературными данными показало, что эти корреляции справедливы в широком диапазоне изменения условий эксперимента: $0{,}1 \leqslant d \leqslant 6{,}0$ мм; $0{,}1 \leqslant p \leqslant 10{,}0$ МПа; $293 \leqslant T_\infty \leqslant 1713$ K; $293 \leqslant T_w \leqslant 1373$ K.